125. Structural Aspects of the Enantioselectivity of Tartrates with α-Amino-alcohol Salts

Part I

Crystal Structures of Eleven Tartaric-Acid Diesters

by **Martin Egli**[1]) and **Max Dobler***

Laboratorium für Organische Chemie, Eidgenössische Technische Hochschule, CH–8092 Zürich

(6.IV.89)

Enantioselective host-guest complexes of α-amino-alcohol salts with chiral tartaric-acid esters can not be crystallised up to now. To study structural aspects of their enantioselectivity, crystal structures of the components were determined. The structures of eleven diesters with myrtanol, borneol, menthol, neomenthol, and *cis*-4-(*tert*-butyl)cyclohexanol in different configurations showed a remarkable rigidity of the tartaric-acid conformation, partly because of intramolecular H-bonding between OH and C=O groups. The conformation of the tartaric-acid part in these diesters is the same as the one observed in optically active tartaric acid (torsion angle O=C–C–OH *ca.* 0°). The binding site for guest molecules is a parallelogram formed by two hydroxy and two carbonyl O-atoms, all lying on the same side of a mean molecular plane. There is one exception: the dimenthyl ester, which is the most enantioselective with a norephedrine guest, has one of the ester groups turned (torsion angle O=C–C–OH *ca.* 180°), forming a triangle of O-atoms and moving the bulky menthyl group to the vicinity of the binding site.

Introduction. – Chiral diesters of tartaric acid show remarkable enantioselectivity with salts of α-amino-alcohols [1][2] and are among the simplest known ionophores. Partition experiments in liquid phases offer a convenient quantitative method to study their enantioselectivity [3].

While the practical possibilities to separate mixtures of stereoisomers have rapidly advanced due to the progress in chromatographic techniques [4], almost nothing is known about the mechanistic aspects of stereoselectivity. The simple and cheap synthesis of tartaric- acid diester hosts and the limited number of possible selectivity parameters led us to a systematic investigation of their stereoselectivity.

The study consists of partition experiments with a vast number of different α-amino-alcohols [2] and tartaric-acid diesters; these results are described in [5]. The molecular complexes formed between the diester hosts and the α-amino-alcohol guests could not be crystallized, so we determined crystal structures of the components separately and used molecular-modeling methods to study possible complex models. In this contribution, we discuss the structures of eleven tartaric-acid diesters and the implications on understanding the structural aspects of their enantioselectivity; a second contribution [6] deals with the structural aspects of α-amino-alcohol guest molecules, and a third discusses molecular-modeling studies [7].

[1]) Present address: Department of Biology, MIT, Cambridge, MA 02139, USA.

Partition Experiments. – Partition experiments with different α-amino-alcohols have shown that the stereogenic C-atom carrying the OH group has a stronger influence on the selectivity than the one carrying the NH_2 group. Without exception, (1*S*)-α-amino-alcohols are preferred by (*R*,*R*)-tartaric-acid diesters and *vice versa*. With (1*S*,2*R*)-norephedrine as reference guest molecule, changes of selectivity as a function of constitution and configuration of different tartaric-acid diesters have been investigated in some 40 cases. The constitution and configuration of alcohol parts with less than eight C-atoms influence the selectivity only to a small extent. The complexes of such esters with norephedrine are relatively stable, but there is only small selectivity compared to esters with higher alcohols, which are more selective but form weaker complexes. Differences in constitution and configuration of the higher alcohols strongly influence the selectivity.

The free enthalpy of selectivity of the di[(1*R*)-menthyl] (*R*,*R*)-tartrate between the norephedrine enantiomers is 0.42 kcal · mol^{-1}, whereas the selectivity of its diastereoisomeric di[(1*S*)-menthyl] (*R*,*R*)-tartrate is 0.20 kcal · mol^{-1}. The highest observed specific enantioselectivity is shown by the di[(1*S*)-neomenthyl] (*R*,*R*)-tartrate. The entropy effect on the selectivity was examined by measuring at different temperatures. The $\Delta\Delta S$ value of the more selective menthyl diester (8 cal · K^{-1} · mol^{-1}) is considerably higher than that of the diastereoisomeric species (3 cal · K^{-1} · mol^{-1}). In this case, therefore, the differences in $\Delta\Delta S$ are mainly responsible for the vast selectivity differences. Generally, diesters with large $\Delta\Delta G$ values also have large $\Delta\Delta S$ values.

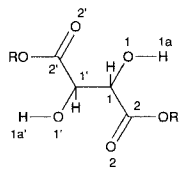

1–11

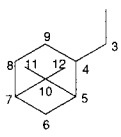

R = Myrtanyl

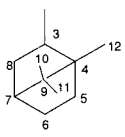

R = Bornyl

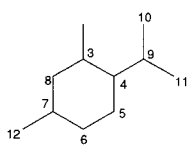

R = Menthyl

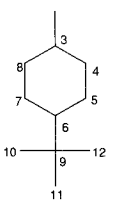

R = *cis*-4-(*tert*-Butyl)cyclohexyl

1 R = (1*S*,2*R*,5*S*)-Myrtanyl ((1*S*,2*R*,5*S*)-6,6-Dimethylbicyclo[3.1.1]heptane-2-methanol)
2* R = (1*R*,2*S*,5*R*)-Myrtanyl ((1*R*,2*S*,5*R*)-6,6-Dimethylbicyclo[3.1.1]heptane-2-methanol)
3* R = (1*R*,2*S*,4*R*)-Bornyl (*endo*-(1*R*,2*S*,4*R*)-1,7,7-Trimethylbicyclo[2.2.1]heptane-2-ol)
4 R = (1*S*,2*R*,4*S*)-Bornyl (*endo*-(1*S*,2*R*,4*S*)-1,7,7-Trimethylbicyclo[2.2.1]heptane-2-ol)
5 R = (1*R*,2*S*,5*R*)-Menthyl ((1*R*,2*S*,5*R*)-5-Methyl-2-(1-methylethyl)cyclohexanol)
6* R = (1*S*,2*R*,5*S*)-Menthyl (1:1 pyridine complex)[2]) ((1*S*,2*R*,5*S*)-5-Methyl-2-(1-methylethyl)cyclohexanol)
7 R = (1*S*,2*R*,5*S*)-Menthyl (1:1 pyridazine complex) ((1*S*,2*R*,5*S*)-5-Methyl-2-(1-methylethyl)cyclohexanol)
8* R = (1*S*,2*S*,5*R*)-Neomenthyl ((1*S*,2*S*,5*R*)-5-Methyl-2-(1-methylethyl)cyclohexanol)
9 R = *cis*-4-(*tert*-Butyl)cyclohexanol
10 R = (1*R*,2*S*,5*R*)-Menthyl (racemic crystal)
11 R = (1*R*,2*S*,5*R*)-Menthyl (tartaric acid O(1) and O(1') methylated; *O*(1), *O*(1')-Dimethyl-**5**)

[2]) Crystals suitable for X-ray crystal structure analysis could not be obtained from the di[(1*S*)-menthyl] ester alone.

Crystallography. – To investigate the principles of complexation of α-amino-alcohols by tartaric-acid diesters, we must know the conformation of the the host molecule. Despite the fact that tartaric-acid diesters are often used in enantioselective syntheses (*e.g.* the important asymmetric epoxidation by *Sharpless* and coworkers [8][9], or the formation of asymmetric C–C bonds [10]), little is known about the influence of varying the alcohol part, and no crystal structures have been reported so far. In the *Cambridge Structural Database* [11], only the structure of dimethyl *meso*-tartrate is deposited. The numbering of the tartaric-acid and alcohol parts used for the crystal structures is shown below. In some cases (marked with an asterisk), the structure analyses were carried out with (*S*,*S*)-tartaric acid; for the sake of consistency, we refer all alcohol configurations to (*R*,*R*)-tartaric acid[3]).

Results. – In all structures, the OH groups of (*R*,*R*)-tartaric-acid diesters are in *M*-synclinal and those of (*S*,*S*)-tartaric-acid diesters in *P*-synclinal orientation. The superposition[4]) of OH and C=O O-atoms of tartaric acid in structures **1**–**9** (**7** is isomorphous with **6** and was not included) shows a remarkable rigidity of this part (*Fig. 1*).

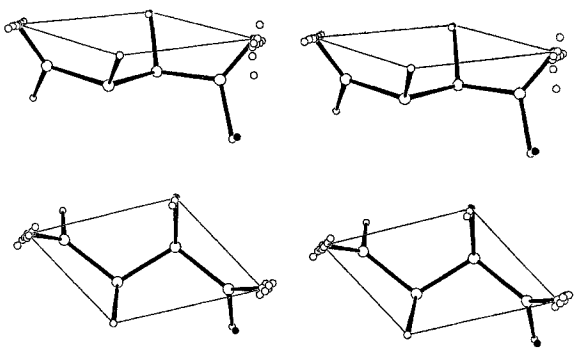

Fig. 1. *Two stereoviews of the superposition of the OH and C=O O-atoms of the tartaric acid from eight different crystal structures (12 cases).* The atom in black corresponds to the position of one of the C=O O-atoms in the di[(1*R*)-menthyl] ester **5**.

In all cases, except **5**, the parallelograms formed by the four O-atoms are very similar (*Table 1*). The ester groups are in the preferred *anticlinal* orientation, with the atoms of a C=O and OH group (carbonyl O, carbonyl C, C(α), hydroxy O) practically in a plane. The tartaric-acid part, thus, has pseudo twofold symmetry (in the case of the pyridine complex **6**, it is crystallographic twofold symmetry). This orientation is also preferred in α-hydroxy-carbonyl compounds, as demonstrated by searching the *Cambridge Structural Database*. *Fig. 2* shows the result with a distinct preference for a torsion angle (HO–C–C=O) of *ca.* 0°.

---

[3]) The numbering of the asymmetric C-atoms corresponds to the systematical nomenclature and differs from the numbering used in the structure analyses.

[4]) The superposition was calculated as follows: the coordinates were transformed to (*R*,*R*)-configuration of tartaric acid. Triangles formed by the two OH and one of the C=O O-atoms were superimposed with one OH O-atom as the common corner and all OH···OH distances along a line. The second C=O O-atom shows characteristic distances from the plane defined by the other three (tartaric-acid C-atoms of one structure added for clarity).

Table 1. *Geometry of the Parallelograms Formed by the OH O-Atoms O(1) and O(1') and the C=O O-Atoms O(2) and O(2') of Tartaric Acid for Eight Diesters* (12 conformations). For structures **2*** and **4**, letters distinguish between the different molecules. In structures with an asterisk, the structure was of the (*S,S*)-tartaric-acid diester, the configurations of the alcohols were transformed to (*R,R*). Distances in Å, angles in degrees. *d*: distance of C=O O(2') from the plane defined by O(1), O(2), and O(1').

Tartrate	Alcohol	O(1)–O(2)	O(2)–O(1')	O(1')–O(2')	O(2')–O(1)	O(1)–O(1')	O(2)–O(2')	Angle at				
								O(1)	O(2)	O(1')	O(2')	*d*
(*R,R*)-**1**	(1*S*)-Myrtanol	2.699(3)	3.507(4)	2.755(4)	3.563(3)	2.841(3)	5.574(4)	125.2(1)	52.6(1)	125.4(1)	51.5(1)	–0.85
(*S,S*)-**2A***	(1*S*)-Myrtanol	2.700(22)	3.112(22)	2.726(22)	3.542(22)	2.964(22)	5.284(22)	115.0(6)	60.8(6)	129.6(7)	54.6(5)	+0.05
(*S,S*)-**2B***	(1*S*)-Myrtanol	2.688(22)	3.423(23)	2.695(23)	3.419(23)	2.923(22)	5.407(23)	124.1(7)	55.6(5)	123.8(7)	55.6(5)	-0.35
(*S,S*)-**3***	(1*S*)-Borneol	2.697(7)	3.138(8)	2.680(8)	3.290(7)	2.996(7)	5.100(8)	116.5(2)	61.2(2)	122.3(3)	59.2(2)	+0.32
(*R,R*)-**4A**	(1*S*)-Borneol	2.683(66)	3.299(63)	2.694(60)	3.345(63)	2.962(63)	5.268(63)	121.4(20)	58.3(15)	122.8(19)	57.5(14)	–0.06
(*R,R*)-**4B**	(1*S*)-Borneol	2.707(60)	3.324(60)	2.629(60)	3.285(60)	2.967(60)	5.222(60)	121.0(18)	57.9(14)	122.2(19)	59.0(14)	+0.05
(*R,R*)-**4C**	(1*S*)-Borneol	2.720(63)	3.330(60)	2.652(63)	3.286(66)	2.958(63)	5.249(63)	121.6(20)	57.5(15)	122.3(19)	58.6(15)	+0.07
(*R,R*)-**4D**	(1*S*)-Borneol	2.695(60)	3.207(60)	2.698(63)	3.316(63)	2.962(60)	5.199(63)	119.4(19)	59.5(14)	123.2(19)	57.9(15)	–0.01
(*R,R*)-**5**	(1*R*)-Menthol	2.647(11)	3.361(10)	3.596(8)	3.251(10)	2.997(10)	5.322(10)	128.5(3)	58.4(2)	99.7(2)	51.6(2)	–1.81
(*S,S*)-**6***[a])	(1*R*)-Menthol	2.666(51)	3.213(51)	2.666(51)	3.213(51)	2.994(51)	5.087(51)	119.6(16)	60.4(12)	119.6(16)	60.4(12)	+0.10
(*S,S*)-**8***	(1*R*)-Neomenthol	2.797(31)	3.494(51)	2.680(31)	3.658(31)	2.796(31)	5.625(31)	120.7(8)	51.3(7)	130.9(7)	49.4(9)	-0.98
(*R,R*)-**9**	*cis*-4-(*tert*-Butyl)-cyclohexanol	2.683(8)	3.373(7)	2.731(7)	3.417(8)	2.949(8)	5.386(6)	123.5(2)	56.9(2)	123.5(2)	56.0(2)	-0.04

[a]) Pyridine complex, pyridazine complex **7** is isomorphous.

Table 2. *Selected Torsion Angles of the Tartaric-Acid Parts in Structures* **1–11** *and Geometry of Intramolecular H-Bonds.* For structures with an asterisk, torsion angles are given for a configuration changed to (*R,R*)-tartaric acid. Diester **6** has a crystallographic twofold rotation axis, **11** has Me groups C(13), C(13') in place of H(1a), H(1a'), and **6** and **7** have disordered H(1a) and H(1a').

	1	**2A***	**2B***	**3***	**4A**	**4B**	**4C**	**4D**	**5**	**6***	**7**
O(1)–C(1)–C(1')–O(1')	–60.5	–76.1	–68.3	–79.0	–68.1	–69.0	–70.5	–68.6	–72.7	–74.6	–75.4
C(2)–C(1)–C(1')–C(2')	–173.0	166.4	176.2	163.7	168.2	168.9	168.3	168.6	171.3	170.7	170.2
O(1)–C(1)– C(2)–O(2)	0.6	13.6	1.6	15.3	10.0	7.8	9.4	10.6	3.4	15.6	7.7
O(1')–C(1')–C(2')–O(2')	1.7	–8.0	1.9	2.7	0.5	7.7	3.0	2.4	–172.5		11.7
C(2)–C(1)–O(1) –H(1a)	–7.2	–7.2	–29.7	–42.0	–71.7	–52.3	–58.1	–30.9	32.1	–72.2	–61.0
C(2')–C(1')–O(1')–H(1a')	–51.1	55.9	–5.3	12.3	–13.0	–40.9	–25.8	–37.0	–71.5		–76.5

	8*	**9**	**10**	**11**
O(1)–C(1)–C(1')–O(1')	–56.9	–77.0	–67.5	–68.1
C(2)–C(1)–C(1')–C(2')	–163.9	168.7	179.8	173.9
O(1)–C(1)– C(2)–O(2)	22.7	–2.4	7.6	0.9
O(1')–C(1')–C(2')–O(2')	–10.9	–2.2	–169.2	3.6
C(2)–C(1)–O(1)–H(1a)	–67.1	–3.6	–43.1	79.4
C(2')–C(1')–O(1')–H(1a')	–16.3	–14.9	–27.0	72.8

Intramolecular H-bonds:

	1	**2A***	**2B***	**3***	**4A**	**4B**	**4C**	**4D**	**5**	**6***	**7**
O(2)···H(1a)	2.241	2.147	2.270	2.405	2.640	2.438	2.491	2.143	2.319	–	–
O(2')···H(1a')	2.573	2.553	2.102	2.199	1.909	2.144	2.070	2.222	–	–	–
O(1)–H(1a)···O(2)	116.1	112.9	102.9	108.8	81.1	91.4	90.5	107.2	100.2	–	–
O(1')–H(1a')···O(2')	93.0	88.4	113.4	123.6	123.4	101.8	111.6	102.9	–	–	–

	8*	**9**	**10**	**11**
O(2)···H(1a)	2.647	2.244	2.509	–
O(2')···H(1a')	1.960	2.295	–	–
O(1)–H(1a)···O(2)	87.4	120.7	96.1	–
O(1')–H(1a')···O(2')	125.3	113.4	–	–

Interestingly, the planarity seems not to be a consequence of internal H-bonding between OH H- and C=O O-atom, because a similar arrangement occurs in the *O,O'*-dimethylated di[(1*R*)-menthyl] ester **11**. Furthermore, examination of the intermolecular H-bonding in the tartaric-acid diester structures reveals no influence on the C(1)–C(2) torsion angle (*Table 2*). We conclude that restriction of this torsion angle to values around 0 and 180° is at best only partly due to internal H-bonding, and that a stereoelectronic effect may be involved as well.

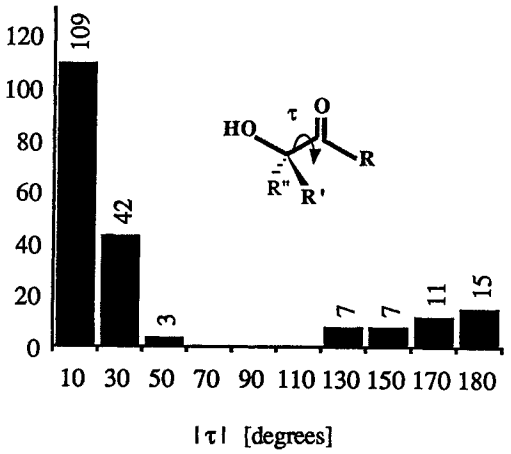

Fig. 2. *Histogram for torsion angle* τ (HO–C–C=O), *in acyclic* α*-hydroxy-carbonyl compounds.* The preference of values around 0 and 180° is obvious.

Recently, *vibrational circular dichroism* spectroscopy was used to investigate the conformations of dimethyl tartrate, diethyl tartrate, and diisopropyl tartrate in solution [12]. The authors reported *anticlinal* orientation of the ester groups and formation of a five-membered ring *via* internal H-bonding. *Ab initio* calculations showed that this H-bond is stabilized by 4 to 8 kcal·mol^{-1} relative to all other possible modes of H-bonding.

Discussion. – With a rather rigid tartaric acid, selectivity must come from the alcohol parts. *Fig. 3* shows the structures of some diesters: di[(1*S*)-bornyl] tartrate (**4**), di[(1*R*)-menthyl] tartrate (**5**), and di[(1*S*)-neomenthyl] tartrate (**8**). The diester **4** shows an enantioselectivity of 0.27 kcal · mol^{-1} with norephedrine, and the measured entropy of selectivity $\Delta\Delta S$ is 4 cal · K^{-1} · mol^{-1}. All tartaric-acid O-atoms lie on the same side of a mean molecular plane, with both bornyl groups pointing into the other direction, resulting in pseudo-twofold symmetry. Even if rotation around the ester C–O bonds is allowed, it is hard to see how the almost spherical bornyl groups can block access to the four O functions of the tartaric acid. On rotation, no part of the bornyl moieties ever rises over the plane through the four O-atoms.

The di[(1*R*)-menthyl] ester **5** is about twice as selective than the dibornyl ester and has a much higher entropy of selection (8 cal · K^{-1} · mol^{-1}). This is also the one exception to the rule of having a C(1)–C(2) torsion angle of *ca.* 0°. One of the torsion angles is *ca.* 180° and causes one of the bulky menthyl groups to lie on the same side as three O-atoms (two OH and a C=O group).

The highest specific enantioselectivity of all investigated compounds is shown by the di[(1*S*)-neomenthyl] ester **8**. Interestingly, in this case the alcohol parts are in a completely different arrangement with the neomenthyl OH group in an axial position. Since, in solution, rotation around the ester C–O bonds is feasible, the i-Pr groups would then be in the direction of the hydrophilic binding site, thus enabling close contacts with the substituents of a guest molecule. This may explain the very high entropy of selectivity of more than 10 cal · K^{-1} · mol^{-1}.

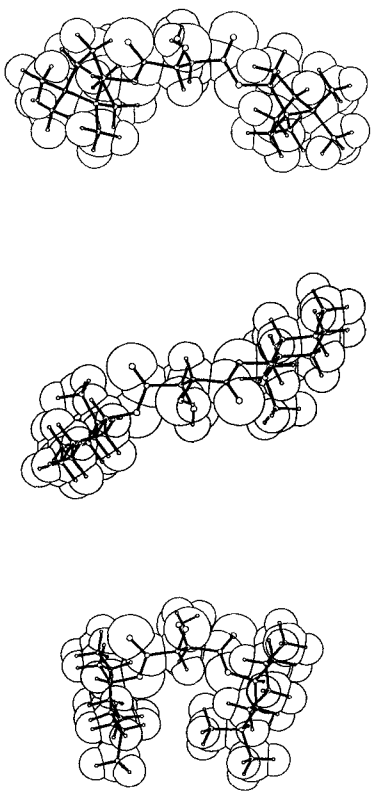

Fig. 3. *Crystal structures of di[(1S)-bornyl] ester* **4**, *di[(1R)-menthyl] ester* **5**, *and di[(1S)-neomenthyl] ester* **8** *in* van der Waals *and ball-and-stick representations*

As already mentioned, the conformation of the di[(1*R*)-menthyl] ester **5** differs from all other cases. The rotation of one ester group by 180° causes the loss of the intramolecular H-bond between OH and C=O group. *Günthard* and coworkers have investigated the IR-induced transformations between the eight possible rotamers of glycolic acid in an Ar matrix [13] (glycolic acid can be regarded as one half of tartaric acid). *Fig. 4* shows two rotamers which are of interest in our context. The first is stabilized by an H-bond, with a measured energy difference of 3.2 kcal · mol^{-1} to the second. We wanted to investigate, whether the different conformation of **5** could be caused by crystal-packing forces.

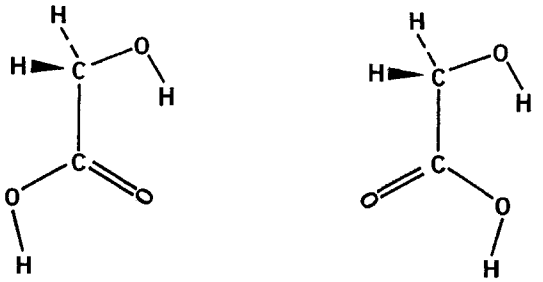

Fig. 4. *Rotamers* 1 (left) *and* 2 *of glycolic acid*

The diastereoisomeric dimenthyl ester **6** could only be crystallized in the form of a 1:1 pyridine complex [14]. In this, the molecule has crystallographic twofold symmetry (*Fig. 5*). The structure is disordered[5]), and, since the N-atom and the C-atom in the 4-position of pyridine are on the rotation axis, two equivalent H-bonds from the N-atom to the OH groups are formed (*Table 5* gives details of the H-bonding geometry).

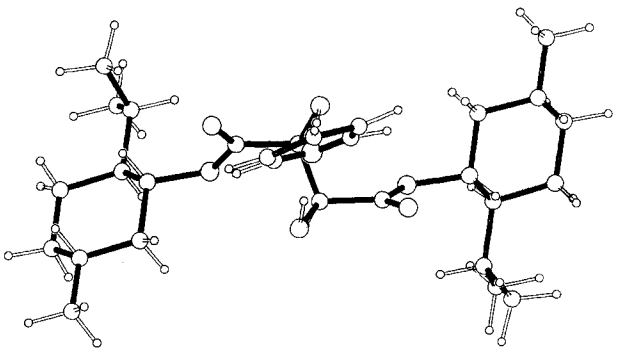

Fig. 5. *Crystal structure of the complex between di[(1*R,2S,5R*)-menthyl] (*S,S*)-tartrate* **6** *and pyridine.* The view is nearly along the twofold axis.

The crystals are quite stable and can be stored for a nearly unlimited time at room temperature. It was also possible to obtain crystals of the di[(1*R*)-menthyl] ester **5** from pyridine[6]). These crystals, however, are unstable at room temperature and turn opaque within hours. It may be assumed that the structures (and possibly the conformation of the diester) differ in the two cases.

---

[5]) The space group symmetry (hexagonal $P6_222/P6_422$) is reduced, when the diester is crystallized from pyridazine (1,2-diazabenzene). The 1:1 pyridazine complex **7** crystallizes in the trigonal space group $P3_121/P3_221$ with pseudo-twofold symmetry. A slight disorder of the solvent molecule is observed.

[6]) 1:1 Clathrate of ester **5** with pyridine: monoclinic $P2_1$, $Z = 2$, cell parameters (precession photographs): $a = 26.45$ Å, $b = 8.02$ Å, $c = 7.05$ Å, $\beta = 92.0°$. The space group is the same indicating that the ester has probably not changed its conformation significantly.

Obviously, diester **5** should be in a completely different environment in a racemic crystal. Also, the two molecules have opposite descriptors of their OH groups with respect to each other. It was mentioned earlier that α-amino-alcohols with (*S*)-configuration at the stereogenic C-atom carrying the OH group are always preferred by (*R*,*R*)-tartrates. (1*S*)-α-Amino-alcohols have *P*-synclinal orientation of OH and ammonium groups, (*R*,*R*)-tartrates *M*-synclinal arrangement of the OH groups. Therefore, one can also state that complexes with complementary descriptors *PM* (or *MP* (= *unlike*)) are more stable than the diastereoisomeric ones with pairs of identical descriptors *PP* (or *MM* (= *like*)). Racemic dimenthyl ester **10** crystallizes in the triclinic space group $P\bar{1}$ with $Z = 2$ (the melting point of the racemate is 57° higher than that of the optically active compound (134° and 77°, respectively)). The conformation of the diesters are very similar to the one in the chiral crystal.

The packing is shown in *Fig.6*. It consists of dimers connected by four H-bonds across a centre of symmetry. The interaction between OH groups are rather weak (O···O-distance = 3.147 Å).

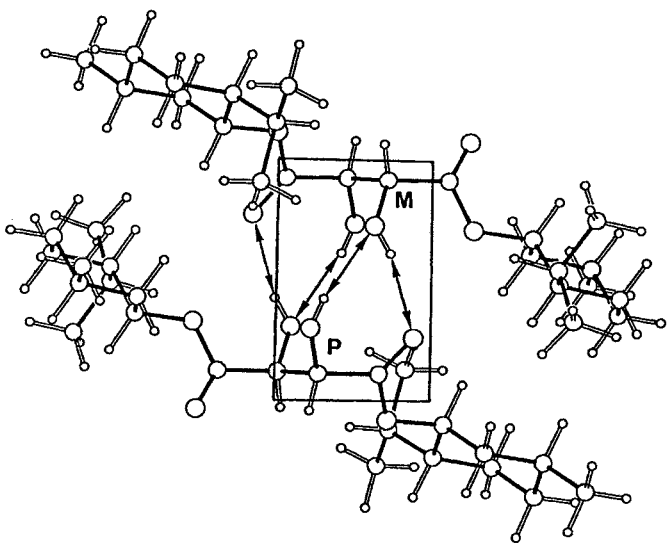

Fig. 6. *Crystal structure of racemic di[(1*R*)-menthyl] ester* **5**. The two molecules are related by a centre of symmetry, the H-bonds are drawn as arrows. The box, with the binding sites of the two molecules and their opposite descriptors, marks the postulated host-guest interaction (O(12) replaced by an ammonium N-atom and the donor hydroxy O-atom O(12) as an acceptor of the ammonium H-atom).

Note, that in this structure there is interaction between two enantiotopic O-atom triangles which we assume to be the sites for binding and recognizing guest molecules! One is tempted to conclude that the geometry of complexes between host and α-amino-alcohol guests could be similar.

Host dimers are also found in the di[(1*S*)-bornyl] ester **4**. The interaction there is between molecules of the same chirality; it is much less favourable and consists of only two H-bonds (*Table 5*).

Experimental Part

Preparation of the Tartrates. Except for di(neomenthyl) ester **8** and di(8-phenylmenthyl) ester (for esterifications with acid-sensitive alcohols an alternative method was developed), the diesters were synthesized according to the procedure given for the di[(1*R*)-menthyl] ester **5** [3]. In some cases, benzene was used instead of toluene as solvent, between 2 and 2.5 equiv. of alcohol[7]) were used, and the amount of MsOH was sometimes increased to 0.2 equiv. The physical properties of all diesters prepared by acid catalysis are summarized in *Table 3*.

Di[(1R,2S,5R)-menthyl] (R,R)-Tartrate (**5**). A mixture of 30 g (0.2 mol) of (+)-(*R,R*)-tartaric acid, 78.1 g (0.5 mol) of (–)-(1*R*,2*S*,5*R*)-menthol, and 2.4 g (0.025 mol) of MsOH in 300 ml of toluene was distilled azeotropically at 140°, until the expected amount of H_2O (7.2 ml) had formed. The mixture was extracted with 5% $NaHCO_3$ (2 × 100 ml), sat. NaCl soln. (2 × 100 ml), and H_2O (2 × 100 ml). Drying of the org. phase ($MgSO_4$) and evaporation yielded a slightly yellow, viscous oil. Menthol was removed at 80° under reduced pressure. The resulting oil (81.8 g) was solved in hot hexane (100 ml). Cooling in the refrigerator yielded 28.8 g of **5** as long colourless needles. R_f (CH_2Cl_2/AcOEt 9:1) 0.87. M.p. 75–77°. $[\alpha]_D$ = –70.6 (*c* = 5, EtOH). ^{1}H-NMR (300 MHz, (D_6)DMSO): 5.29 (*d*, *J* = 8, 2 CH(O*H*)COOR); 4.61 (*dt*, *J* = 4, 11, 2 C*H*OR); 4.33 (*d*, *J* = 8, 2 C*H*(OH)COOR).

Di(neomenthyl) Tartrates. Preparation of Di[(1R,2R,5S)-neomenthyl] Fumarate. (–)-(1*R*,2*R*,5*S*)-neomenthol (9.11 g, 0.058 mol) and $NaHCO_3$ (4.9 g, 0.058 mol) were placed in a dry flask, and 200 ml of toluene were added. Under stirring, 4.13 g (2.9 ml, 0.027 mol) fumaroyl dichloride were added, and the mixture was refluxed for 30 h at 145°. The soln. was extracted with 5% $NaHCO_3$ and sat. NaCl soln. Drying of the org. phase ($MgSO_4$) and evaporation of the solvent yielded a crystalline product which was recrystallized from hexane/EtOH at –20°: 7.2 g (0.018 mol, 68%) of colourless crystalline di[(1*R*,2*R*,5*S*)-neomenthyl) fumarate. R_f (hexane/AcOEt 2:1) 0.89. M.p. 82–84°. $[\alpha]_D$ = –39.2 (*c* = 5, EtOH). ^{1}H-NMR (300 MHz, $CDCl_3$): 6.81 (*s*, 2 C*H*COOR); 5.33 (br. *d*, *J* = 2, C*H*OR).

Oxidation of the Fumarate. Fumarate (1 g, 2.55 mmol) was solved in 10 ml of acetone in a dry flask under N_2. After addition of 166 mg (0.64 mmol, 0.25 equiv.) of Et_4NOAc (4 H_2O) and 0.54 ml (372 mg, 4.12 mmol, 1.6 equiv.) of *t*-BuOOH, the soln. was stirred, until the acetate had dissolved completely. The soln. was cooled with ice, and 0.26 ml of OsO_4 catalyst [22] were added in one portion. The cooling bath was removed after 45 min, and the soln. was stirred over night. The mixture was cooled again, and 10 ml of Et_2O were added. After the addition of 1.5 ml of 10% $NaHSO_3$, the ice bath was removed, and the mixture was stirred for 1 h, until the org. phase had completely decoloured. After saturation of the purple H_2O phase with NaCl, the org. layer was separated and once extracted with H_2O and dried ($MgSO_4$). Evaporation of the solvent yielded 1 g (2.34 mmol, 92%) of crystalline mixture of the diastereoisomeric tartrates. M.p. 125°. Recrystallizing the mixture three times (EtOH/H_2O) had no influence on the m.p. Transformation to the corresponding acetonide was not advantageous regarding the separation of the diastereoisomers. The isomers could be separated by prep. HPLC[8]) (column: *KNAUER-Lichosorb* 7µm, silica gel, solvent: heptane/*t*-BuOMe 20:1, 50 ml/min, 0.6 MPa, UV detection at 225 nm). Separation of 1.2 g of the mixture of the diastereoisomers (100-mg fractions) yielded 495 mg of di[(1*R*,2*R*,5*S*)-neomenthyl] (*R,R*)-tartrate (colourless oil; $[\alpha]_D$ = +23.9 (*c* = 1, EtOH). ^{1}H-NMR (300 MHz, $CDCl_3$): 5.37 (*d*, *J* = 2, 2 C*H*OR); 4.44 (*d*, *J* = 6, 2 C*H*(OH)COOR); 3.10 (*d*, *J* = 6, 2 CH(O*H*)COOR)) and 485 mg of di[(1*R*,2*R*,5*S*)-neomenthyl] (*S,S*)-tartrate (**8**; crystalline; m.p. 108–110°; $[\alpha]_D$ = –57.5 (*c* = 1, EtOH). ^{1}H-NMR (300 MHz, $CDCl_3$): 5.36 (*d*, *J* = 2, 2 C*H*OR); 4.47 (*d*, *J* = 7, 2 C*H*(OH)COOR); 3.08 (*d*, *J* = 7, 2 CH(O*H*)COOR)). The ester configurations were checked with by independent methods: saponification of one of the esters and measurement of the specific rotation of the formed tartaric acid, consistency with the *like-unlike* rule from the partition experiments, and finally with the X-ray analysis of **8**.

Di(8-phenylmenthyl) Tartrates. The fumarate was prepared following the procedure for the neomenthyl ester: 5.71 g (0.025 mol) of (1*R*,2*S*,5*R*)-8-phenylmenthol ($[\alpha]_D$ = –22 (*c* = 1, EtOH)) and 1.87 g (0.012 mol) of fumaroyl dichloride gave 5.77 g (0.011 mol, 87%) of diester as colourless glass after chromatography (hexane/AcOEt 9:1, R_f 0.50). M.p. 115–120°. $[\alpha]_D$ = –10.4 (*c* = 1, EtOH). ^{1}H-NMR ($CDCl_3$): 7.22 (*m*, 8 arom. H); 7.07 (*m*, 2 arom. H); 5.76 (*s*, 2 C*H*COOR); 4.85 (*dt*, *J* = 4, 11, 2 C*H*OR).

---

[7]) *cis*-4-(*tert*-Butyl)cyclohexanol is commercially available as a mixture of the *cis*- and the *trans*-isomers (33% *cis*, 67% *trans*). The isomers were separated chromatographically (silica gel, CH_2Cl_2/AcOEt 4:1, R_f(*trans*-isomer) 0.42 and R_f(*cis*- isomer) 0.56). The isomers were identified by their different IR absorption between 850 and 1150 cm^{-1} [15] (C–O_{st}, 2% solns. in CCl_4). Due to the axial position of the OH group in the *cis*-isomer, the diester is obtained in very low yields.

[8]) We thank Dr. *J. Schreiber* from the Laboratorium für organische Chemie, ETH Zürich, for the analytical separation of the diastereoisomers.

... $CDCl_3$ was used normally (300 MHz). For esters prepared according to other procedures, the corresponding reference is given.

Tartaric Acid	Alcohol	Diester	Ref.	Purification	M.p.	$[\alpha]_D$	^{1}H-NMR		
							δ(OH)	δ(R^{1}C*H*(OH)COOR)	δ(R^{1}CH(O*H*)COOR)
(*R*,*R*)	(*S*)-2-Methyl-butanol	–	[16]	Dest. 195°/0.08Torr	–	+20.3 (*c* = 5, EtOH)	5.40 (*d*, 2 H)	4.40 (*d*, *J* = 8, 2 H)	4.00 (*dd*, *J* = 8, 6, 2 H); 3.88 (*dd*, *J* = 8, 7, 2 H)[a])
(*S*,*S*)	(*S*)-2-Methyl-butanol	–	[16]	Dest. 195°/0.03Torr	–	–10.9 (*c* = 5, EtOH)	5.41 (*d*, 2 H)	4.40 (*d*, *J* = 8, 2 H)	3.94 (*dd*, *J* = 2, 6, 4 H)[a])
(*R*,*R*)	1-Octanol	–	[17]	Dest. 165°/0.015Torr	43	+8.4 (*c* = 5, EtOH)	3.16 (*d*, 2 H)	4.53 (*d*, *J* = 6, 2 H)	4.26 (*dt*, *J* = 1, 7, 4 H)
(*R*,*R*)	(*R*)-2-Octanol	–	[18]	Dest. 165°/0.03Torr	–	–3.3 (*c* = 2, EtOH)	3.25 (br. *s*, 2 H)	4.48 (*s*, 2 H)	5.07 (*m*, 2 H)
(*R*,*R*)	(*S*)-2-Octanol	–	[18]	Dest. 160°/0.02Torr	–	+20.4 (*c* = 5, EtOH)	3.70 (br. *s*, 2 H)	4.49 (*s*, 2 H)	5.07 (*m*, 2 H)
(*R*,*R*)	1-Nonanol	–	–	Dest. 180°/0.01Torr	49–50	+10.2 (*c* = 1.73, MeOH)	3.14 (br. *s*, 2 H)	4.53 (*s*, 2 H)	4.26 (*dt*, *J* = 1, 7, 4 H)
(*R*,*R*)	5-Nonanol	–	–	Dest. 165°/0.08Torr	–	+9.8 (*c* = 5, EtOH)	3.10 (br. *s*, 2 H)	4.50 (*s*, 2 H)	5.04 (*m*, 2 H)
(*R*,*R*)	Cyclopentanol	–	–	Dest. 100°/0.01Torr	–	+20.0 (*c* = 5, EtOH)	3.80 (br. *s*, 2 H)	4.45 (*s*, 2 H)	5.32 (*m*, 2 H)
(*R*,*R*)	Cyclohexanol	–	–	Recryst. hexane	58–60	+14.2 (*c* = 5, EtOH)	3.14 (*d*, 2 H)	4.50 (*d*, *J* = 6, 2 H)	4.92 (*m*, 2 H)
(*R*,*R*)	Benzyl alcohol	–	[19]	Recryst. toluene	50	+7.8 (*c* = 5, EtOH)	5.62 (*d*, 2 H)	4.53 (*d*, *J* = 8, 2 H)	5.16 (*s*, 4 H)[a])
(*R*,*R*)	(1*R*,2*S*,4*S*)-Fenchol	–	–	Recryst. hexane	124–126	+54.9 (*c* = 5, EtOH)	5.35 (br. *s*, 2 H)	4.35 (*d*, *J* = 2, 2 H)	4.47 (*s*, 2 H)[a])
(*S*,*S*)	(1*R*,2*S*,4*S*)-Fenchol	–	–	Chrom. CH_2Cl_2/AcOEt 9:1	–	+39.0 (*c* = 2, EtOH)	2.67 (br. *s*, 2 H)	4.54 (*s*, 2 H)	4.54 (*s*, 2 H)
(*R*,*R*)	(1*S*,2*R*,5*S*)-Myrtanol	**1**	–	Recryst. EtOH	78–80	–3.3 (*c* = 5, EtOH)	5.39 (*d*, 2 H)	4.36 (*d*, *J* = 8, 2 H)	4.03 (*m*, 4 H)[a])
(*S*,*S*)	(1*S*,2*R*,5*S*)-Myrtanol	**2**	–	Recryst. EtOH	87–89	–26.4 (*c* = 5, EtOH)	3.13 (*d*, 2 H)	4.51 (*d*, *J* = 8, 2 H)	4.28, 4.16 (*dd*, *J* = 8, 8, 2 H)
(*S*,*S*)	(1*S*,2*R*,4*S*)-Borneol	**3**	[20]	Dest. 220°/0.01Torr	114–115	–63.2 (*c* = 5, EtOH)	3.13 (*d*, 2 H)	4.56 (*d*, *J* = 4, 2 H)	5.02 (*m*, 2 H)
(*R*,*R*)	(1*S*,2*R*,4*S*)-Borneol	**4**	[20]	Dest. 200°/0.01Torr	130–131	–12.4 (*c* = 5, EtOH)	3.15 (*d*, 2 H)	4.55 (*d*, *J* = 7, 2 H)	5.15 (*m*, 2 H)
(*R*,*R*)	(1*R*,2*S*,5*R*)-Menthol	**5**	[21]	Recryst. hexane	75–77	–70.6 (*c* = 5, EtOH)	5.29 (*d*, 2 H)	4.33 (*d*, *J* = 8, 2 H)	4.61 (*dt*, *J* = 4, 11, 2 H)[a])
(*R*,*R*)	(1*S*,2*R*,5*S*)-Menthol	**6**	[14]	Pyridine complex	41–43	+80.6 (*c* = 5, EtOH)	5.39 (*d*, 2 H)	4.33 (*d*, *J* = 8, 2 H)	4.66 (*dt*, *J* = 4, 11, 2 H)[a])
(*R*,*R*)	(1*S*,2*R*,5*R*)-Isomenthol	–	–	Recryst. EtOH/H_2O	126	+31.6 (*c* = 1, EtOH)	3.12 (*d*, 2 H)	4.49 (*d*, *J* = 7, 2 H)	5.20 (*m*, 2 H)
(*S*,*S*)	(1*S*,2*R*,5*R*)-Isomenthol	–	–	Recryst. EtOH/H_2O	64–66	+12.1 (*c* = 1, EtOH)	3.16 (*d*, 2 H)	4.49 (*d*, *J* = 7, 2 H)	5.20 (*m*, 2 H)
(*R*,*R*)	*cis*-4-(*tert*-Butyl)-cyclohexanol	**9**	–	Recryst. CH_2Cl_2/pentane	134–136	+16.8 (*c* = 1, EtOH)	3.13 (*d*, 2 H)	4.45 (*d*, *J* = 6, 2 H)	5.17 (*m*, 2 H)
(*R*,*R*)	*trans*-4-(*tert*-Butyl)-cyclohexanol	–	–	Recryst. CH_2Cl_2/pentane	181–183	+4.3 (*c* = 0.5, EtOH)	3.09 (*d*, 2 H)	4.47 (*d*, *J* = 8, 2 H)	4.79 (*m*, 2 H)
(*R*,*R*)	3,3,5,5-Tetramethyl-cyclohexanol	–	–	Recryst. EtOH/H_2O	109	+8.1 (*c* = 1, EtOH)	3.16 (*d*, 2 H)	4.46 (*d*, *J* = 7, 2 H)	5.20 (*m*, 2 H)
(*R*,*R*)	(1*R*,2*S*)-2-Phenyl-cyclohexyl	–	–	Chrom. CH_2Cl_2/AcOEt 9:1	110–140	–39.7 (*c* = 2, EtOH)	2.04 (*d*, 2 H)	3.55 (*d*, *J* = 8, 2 H)	4.95 (*dt*, *J* = 5, 11, 2 H)
(*S*,*S*)	(1*R*,2*S*)-2-Phenyl-cyclohexyl	–	–	Recryst. EtOH/H_2O	100–130	–33.5 (*c* = 2, EtOH)	2.75 (*d*, 2 H)	4.04 (*d*, *J* = 7, 2 H)	5.08 (*dt*, *J* = 4, 11, 2 H)
(*R*,*R*)	Cyclododecanol	–	–	Recryst. toluene	111–112	+8.6 (*c* = 1, EtOH)	3.13 (*d*, 2 H)	4.46 (*d*, *J* = 7, 2 H)	5.16 (*m*, 2 H)
(*R*,*R*)	Adamantanol	–	–	Recryst. MeOH	156–160	+7.6 (*c* = 1, EtOH)	2.45 (br. *s*, 2 H)	4.36 (*s*, 2 H)	–

[a]) ^{1}H-NMR in (D_6)DMSO.

Di[(1*R*,2*S*,5*R*)-8-phenylmenthyl] fumarate (2.5 g, 0.0046 mol) was solved in 50 ml of acetone. The soln. was cooled with ice, and 800 mg (1.1 equiv.) of $KMnO_4$ in 60 ml of acetone were added slowly over a period of 2 h. The ice bath was removed and the mixture was stirred at r.t. for 1 h. Et_2O (200 ml) and 50 ml of 10% $NaHSO_3$ were then added, and the mixture was stirred, until the org. layer had completely decoloured. The H_2O layer was saturated with NaCl, the org. layer was separated and once extracted with H_2O and dried ($MgSO_4$). Evaporation of the solvent gave 2.15 g (81%) of crystalline oxidation product which was chromatographed ($MeCl_2$/AcOEt 19:1) to furnish 0.58 g of di[(1*R*,2*S*,5*R*)-8-phenylmenthyl] (*S*,*S*)-tartrate (m.p. 147–149°. $[\alpha]_D = -3.5$ (*c* = 1, EtOH). ^{1}H-NMR ($CDCl_3$): 4.91 (*dt*, *J* = 4, 11, 2 *CH*OR); 3.73 (*s*, 2 *CH*(OH)COOR); 2.60 (br. *s*, 2 CH(O*H*)COOR). FAB-MS: 601 ([*M* + Na]$^+$). Anal. calc. for $C_{36}H_{50}O_6$ (578.79): C 74.71, H 8.71; found: C 74.77, H 8.75) and 0.55 g of di[(1*R*,2*S*,5*R*)-8-phenylmenthyl] (*R*,*R*)-tartrate. (M.p. 57–60°; $[\alpha]_D = -3.7$ (*c* = 1, EtOH); ^{1}H-NMR ($CDCl_3$): 4.90 (*dt*, *J* = 4, 11, 2 *CH*OR); 3.94 (*d*, *J* = 3, 2 *CH*(OH)COOR); 2.07 (*d*, *J* = 3, 2 CH(O*H*)COOR). FAB-MS: 601 [*M* + Na]$^+$. Anal. calc. for $C_{36}H_{50}O_6$ (578.79): C 74.71, H 8.71; found: C 74.49, H 8.77). The ester configurations were checked by saponification and measurement of the specific rotations of the resulting tartaric acids and confirmed by consistency with the *like-unlike* rule from the partition experiments.

X-Ray Crystallography. – *General.* Space groups and approximate cell parameters were determined from precession photographs for all structures. The reflection intensities were measured at r.t. on a four-circle diffractometer *Enraf-Nonius CAD4*, equipped with a graphite monochromator: $\lambda(MoK_\alpha) = 0.71069$ Å. The cell constants were refined with at least eight reflections with $\theta > 8°$, and the reflections were measured with ω scans (using two reflections for intensity control every 10000 s and three reflections for orientation control every 100 reflections). The intensities were corrected for *Lorentz* and polarisation effects, absorption corrections were not applied. Except for **4** and **7**, the structures were solved by direct methods with SHELX-84 [23] or SHELXS-86 [24], refinements with programs SHELX-76 [25] or XRAY [26] (for **2** and **4** with large numbers of parameters). Heavy atoms (C, O, N) were refined anisotropically except for **4** and **8** (isotropic). The positions of the H-atoms attached to C-atoms were calculated for all structures and refined using constraints: H-atoms fixed at a distance of 1.08 Å, displacement parameters restricted to 120% of $(U_{11}+U_{22}+U_{33})/3$ of the corresponding C-atom. For di[(1*S*)-myrtanyl] ester **1**, the H-positions were refined isotropically, but their displacement parameters were restricted as described above. The positions of the OH H-atoms were usually determined from difference *Fourier* maps and refined isotropically, sometimes restricting their displacement parameters. In **2**, three of the four OH H-atoms could not be refined. In cases of short contacts between two O-atoms, the following criteria to calculate the H-positions were applied: angle at the H-atom as linear as possible, distance between H and acceptor as short as possible, and angle between the direction defined by H, acceptor, and acceptor lone pair as small as possible. The H-atoms were then placed at 1 Å from the corresponding O-atoms with C–O–H-angles of 109° and arbitrary C–C–O–H torsion angles. On a graphics computer, the torsion angles were set to reasonable values according to the above rules. The positions were then fixed during refinement. In **4**, the position of only one of the four H-atoms of OH groups was seen in a difference *Fourier* map. The same procedure as for the di[(1*S*)-myrtanyl] ester **2** was used to calculate the H-positions. Only for diester **3**, weights ($1/\sigma^2$) were applied during refinement, all other structures were refined with unit weights. *Table 4* contains crystal data for structures **1–11,** details of the H-bond geometries are given in *Table 5*.

*Di[(1S,2R,4S)-bornyl] (*R,R*)-Tartrate* (**4**). The structure could not be solved with direct methods (four independent ester molecules with a total of 120 C- and O-atoms in the asymmetric unit). With a computer-generated dibornyl ester model with a free torsion around one of the ester bonds as search fragment, a *Patterson* search with the program PATSEE [27] and a tangent refinement with the rotationally and translationally correctly positioned fragment gave two of the four molecules (**A** and **B**). Molecules **C** and **D** were then located with four difference *Fourier* maps. The structure was refined isotropically, the H-positions were calculated and treated with an overall isotropic temperature factor $U = 0.1$. The four molecules adopt nearly identical conformations (*Table 2* and *Fig. 7*) which facilitated the *Patterson* search. Two dimers, one between molecules **A** and **B** and the other between molecules **C** and **D** are formed, and both are connected over two H-bonds (see *Table 5* for the geometry). The two dimers **A**, **B** and **C**, **D** adopt identical orientations in the unit cell, separated by a translation vector with components (0.191, 0.607, 0.316) along the cell axes.

*Di[(1S,2R,5S)-menthyl] (*R,R*)-Tartrate Pyridazine Complex* (**7**). The structure could neither be solved with direct methods nor in combination with *Patterson* searches. A *Fourier* synthesis with the coordinates of the pyridine complex did not lead to any refineable fragments. Since the cell constants of the hexagonal pyridine complex **6** and the trigonal pyridazine complex **7** are very similar (*Table 4*) and the intensities of the *hk0* reflections of the two structures showed a similar pattern, the projections along the *c* axis had to be similar. When the *x* and *y* coordinates of **6** and of its enantiomer were shifted with a step size of 0.05 along the *c* axis in the $P3_121$ cell of the pyridazine complex (diastereomorphic relation), a minimum for the *R* factor was reached at $z = 0.34$. For this

procedure, a restricted data set was used ($\theta < 11°$). During refinement, starting with the raw coordinates, the alcohol parts were at first kept fixed, and the number of reflections was increased every cycle until an R factor of 0.12 was reached.

The projections along the c axes of **6** and **7** are very similar. Ester and solvent molecule have twofold symmetry in **6**, the ester molecule in **7** adopts only pseudo twofold symmetry.

Full lists of coordinates and anisotropic displacement parameters as well as H-positions for all structures are deposited at the *Cambridge Structural Data Centre* and are available upon request from the authors.

Table 4. *Crystal Data for Structures* **1–11**. In the second solvent, the compounds were only slightly soluble or insoluble. A number with an asterisk indicates (*S,S*)-tartaric acid. R factors: i = isotropic refinement, w = weighted refinement ($1/\sigma^2$).

Compound	**1**	**2***	**3***	**4**	**5**
Formula	$C_{24}O_6H_{38}$	$C_{24}O_6H_{38}$	$C_{24}O_6H_{38}$	$C_{24}O_6H_{38}$	$C_{24}O_6H_{42}$
Crystallization	EtOH, 5°	EtOH, 5°	hexane, r.t.	CH_2Cl_2, r.t.	EtOH/H_2O, r.t.
Space group	$P2_1$	$P2_1$	$P2_1$	$P1$	$P2_1$
Crystal system	monoclinic	monoclinic	monoclinic	triclinic	monoclinic
a [Å]	10.145(6)	12.244(8)	10.133(6)	12.928(6)	16.349(7)
b [Å]	6.468(3)	12.355(12)	7.123(6)	13.832(14)	5.537(1)
c [Å]	18.322(7)	16.331(8)	17.289(11)	15.296(13)	14.250(6)
α [°]	–	–	–	71.32(7)	–
β [°]	101.93(4)	106.60(5)	98.28(5)	64.89(5)	98.62(3)
γ [°]	–	–	–	81.80(6)	–
V [Å^3]	1176.2	2367.6	1234.8	2346.0	1275.3
Z	2	4	2	4	2
ρ_{calc} [g·cm^{-3}]	1.19	1.19	1.14	1.20	1.11
θ_{max} [°]	28	25	24	23	23
Unique refl.	3086	4369	2122	6517	1975
Refl. $I > 3\sigma(I)$	2231	3424	1366	2702	1366
R factor	0.042 w	0.056	0.043	0.13 i	0.047

Compound	**6***	**7**	**8***	**9**	**10**	**11**
Formula	$C_{24}O_6H_{42}$ C_5H_5N	$C_{24}O_6H_{42}$ · $C_4H_4N_2$	$C_{24}O_6H_{42}$	$C_{24}O_6H_{42}$	$C_{24}O_6H_{42}$	$C_{26}O_6H_{46}$
Crystallization	pyridine, 5°	pyridazine, 0°	EtOH/H_2O, r.t.	CH_2Cl_2/pentane, –20°	EtOH/H_2O, r.t.	EtOH/H_2O, 5°
Space group	$P6_222/P6_422$	$P3_121/P3_221$	$P2_1$	$P2_12_12_1$	$P\bar{1}$	$P2_12_12_1$
Crystal system	hexagonal	trigonal	monoclinic	orthorhombic	triclinic	orthorhombic
a [Å]	18.95(1)	18.864(3)	13.331(5)	9.094(2)	9.711(4)	8.869(3)
b [Å]	–	-	6.358(3)	11.756(7)	9.894(3)	9.357(4)
c [Å]	15.939(4)	15.764(6)	15.467(19)	23.451(10)	14.483(3)	34.100(11)
α [°]	–	–	–	–	82.94(2)	–
β [°]	–	–	109.03(5)	–	82.40(3)	–
γ [°]	–	–	–	–	64.24(2)	–
V [Å^3]	4958.0	4857.7	1239.3	2507.0	1238.9	2835.4
Z	6 (1:1 complex)	6 (1:1 complex)	2	4	2	4
ρ_{calc} [g·cm^{-3}]	1.02	1.04	1.14	1.13	1.14	1.07
θ_{max} [°]	22	25	25	25	25	23
Unique refl.	1248	3115	2391	2506	4354	2286
Refl. $I > 3\sigma(I)$	445	1052	761	1577	2813	1256
R factor	0.12	0.084	0.11 i	0.041	0.048	0.041

Table 5. *Intermolecular H-Bond Geometry.* Distances in Å and angles in degrees. E.s.d. in parentheses refer to the last digit.

	H-Bond	*d* (O···O)	*d* (O···H)	Angle (O–H···O)	Symmetry operation
1	O(1)···H(1')–O(1')	3.001(3)	2.16(4)	167(4)	(2–*x*, 1/2+*y*, 1–*z*)
	O(1)–H(1)···O(2')	2.862(3)	2.18(4)	142(4)	(2–*x*, 1/2+*y*, 1–*z*)
2	(O(1')–H(1'))a···O(2)b	2.92(2)	1.98	151	–
	O(1)a···(H(1)–O(1))b	3.05(2)	2.06	164	(–*x*, *y*–1/2, 2–*z*)
3	O(1)–H(1)···O(2')	2.816(7)	2.22(6)	150(6)	(2–*x*, *y*–1/2, –*z*)
4	(O(1')–H(1'))a···O(2)b	2.83	2.00	128	–
	O(2')a···(H(1)–O(1))b	2.85	1.87	144	–
	(O(1')–H(1'))c···O(2)d	2.90	2.03	137	–
	O(2')c···(H(1)–O(1))d	2.91	1.94	143	–
5	O(1')–H(1')···O(2')	2.960(2)	2.138(4)	148(3)	(*x*, 1+*y*, *z*)
6	O(1)–H(1)···N(1)p	2.87(10)		structure disordered	–
7	O(1)–H(1)···N(1)p	2.77(3)	1.64(20)	177(>10)	–
	O(1')–H(1')···N(1)p	3.04(3)	1.93(20)	172(>10)	–
8	O(2)···H(1')–O(1')	2.81(3)	2.24(3)	114(2)	(2–*x*, *y*–1/2, 1–*z*)
	O(1)–H(1)···O(1')	3.01(3)	2.05(3)	155(2)	(2–*x*, *y*–1/2, 1–*z*)
9	O(1)···H(1')–O(1')	2.874(8)	2.21(8)	138(7)	(*x*–1/2, 1.5–*y*, 1–*z*)
	O(1)–H(1)···O(2')	2.812(8)	2.38(7)	120(7)	(*x*–1/2, 1.5–*y*, 1–*z*)
10	O(1)–H(1)···O(1')	3.148(5)	2.35(8)	167(8)	(–*x*, –*y*, –*z*)
	O(2)···H(1')–O(1')	2.839(4)	2.09(5)	162(5)	(–*x*, –*y*, –*z*)

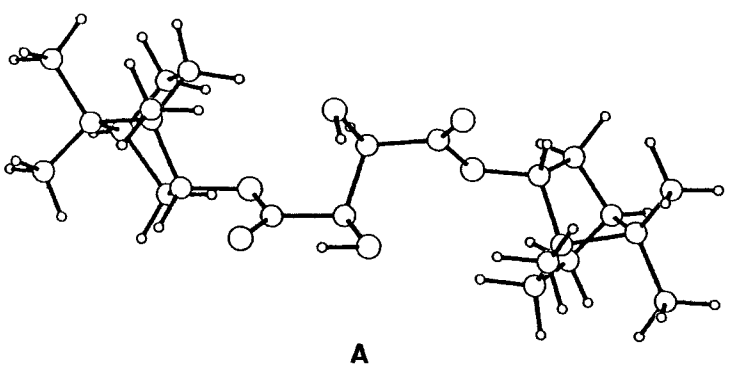

Fig. 7. *Projection of one of the four molecules along the pseudo twofold axis.* The other three crystallographically independent molecules adopt almost superimposable conformations.

REFERENCES

[1] V. Prelog, S. Mutak, K. Kovacevic, *Helv. Chim. Acta* **1983**, *66*, 2279.
[2] V. Prelog, M. Dumic, *Helv. Chim. Acta* **1986**, *69*, 5.
[3] V. Prelog, Z. Stojanac, K. Kovacevic, *Helv. Chim. Acta* **1982**, *65*, 377.
[4] S.G. Allenmark, 'Chromatographic Enantioseparation: Methods and Applications', Ellis Horwood Ldt., Chichester, 1988.

[5] a) M. Egli, ETH-Dissertation No. 8729, 1988; b) V. Prelog, M. Egli, M. Kovacevic, submitted to *Angew. Chem.*
[6] M. Egli, M. Dobler, *Helv. Chim. Acta* **1989**, *72*, 1151.
[7] M. Egli, M. Dobler, *Helv. Chim. Acta*, in preparation.
[8] T. Katsuki, K. B. Sharpless, *J. Am. Chem. Soc.* **1980**, *102*, 5974.
[9] C. H. Behrens, K. B. Sharpless, *Aldrichim. Acta* **1983**, *16*, 67.
[10] R. Haruta, M. Ishiguro, N. Ikeda, H. Yamamoto, *J. Am. Chem. Soc.* **1982**, *104*, 7667.
[11] F. H. Allen, S. Bellard, M. D. Brice, B. A. Cartwright, A. Doubleday, H. Higgs, T. Hummelink, B. G. Hummelink-Peters, O. Kennard, W. D. S. Motherwell, J. R. Rodgers, D. G. Watson, *Acta Crystallogr., Sect. B* **1979**, *35*, 2331.
[12] P. L. Polavarapu, C. S. Ewig, T. Chandramouly, *J. Am. Chem. Soc.* **1987**, *109*, 7382.
[13] H. Hollenstein, T.-K. Ha, H. H. Günthard, *J. Mol. Struct.* **1986**, *146*, 289.
[14] T. S. Patterson, J. Kaye, *J. Chem. Soc.* **1906**, *89* 1884.
[15] R. A. Pickering, C. C. Price, *J. Am. Chem. Soc.* **1958**, *80*, 4931.
[16] P. Walden, *Z. Phys. Chem.* **1895**, *17*, 705.
[17] P. F. Frankland, F. H. Garner, *J. Chem Soc.* **1919**, *115*, 636.
[18] R. H. Pickard, J. Kenyon, *J. Chem. Soc.* **1911**, *99*, 45.
[19] T. S. Patterson, *J. Chem. Soc.* **1913**, *103*, 176.
[20] H. Wren, H. Williams, W. W. Myddleton, *J. Chem. Soc.* **1920**, *117*, 191.
[21] T. S. Patterson, F. Taylor, *J. Chem. Soc.* **1905**, *87*, 33.
[22] K. Akashi, R.E. Palermo, K.B. Sharpless, *J.Org.Chem.* **1978**, *43*, 2063.
[23] G. M. Sheldrick, SHELX-84, unpublished version.
[24] G. M. Sheldrick, SHELXS-86, 'Crystallographic Computing 3', Eds. G. M. Sheldrick, C. Krüger, and R. Goddard, Oxford University Press, Oxford, 1985, p. 175.
[25] G. M. Sheldrick, SHELX-76, System of Computing Programmes, University of Cambridge, Cambridge, England.
[26] J. M. Stewart, G. J. Krüger, H. L. Ammon, C. Dickinson, S. R. Hall, The X-RAY SYSTEM, Computer Science Center, University of Maryland, College Park, Maryland, 1972.
[27] E. Egert, G. M. Sheldrick, *Acta Crystallogr., Sect. A* **1985**, *41*, 262.